

RSC Advances



This is an *Accepted Manuscript*, which has been through the Royal Society of Chemistry peer review process and has been accepted for publication.

Accepted Manuscripts are published online shortly after acceptance, before technical editing, formatting and proof reading. Using this free service, authors can make their results available to the community, in citable form, before we publish the edited article. This *Accepted Manuscript* will be replaced by the edited, formatted and paginated article as soon as this is available.

You can find more information about *Accepted Manuscripts* in the [Information for Authors](#).

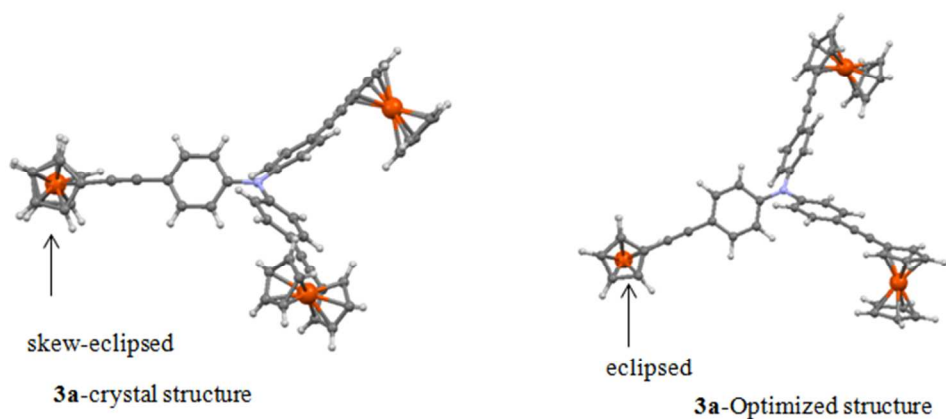
Please note that technical editing may introduce minor changes to the text and/or graphics, which may alter content. The journal's standard [Terms & Conditions](#) and the [Ethical guidelines](#) still apply. In no event shall the Royal Society of Chemistry be held responsible for any errors or omissions in this *Accepted Manuscript* or any consequences arising from the use of any information it contains.

Star Shaped Ferrocenyl Substituted Triphenylamines

Rajneesh Misra*, Ramesh Maragani, Biswarup Pathak, Prabhat Gautam, Shaikh M. Mobin

Department of Chemistry, Indian Institute of Technology Indore, Indore 452017, India

TOC



ABSTRACT

This manuscript reports design and synthesis of Star shaped ferrocenyl substituted triphenylamine conjugates (Fc-TPA) **3a–3c** by the Pd-catalyzed Sonogashira cross-coupling reaction. Their photophysical, and electrochemical properties were investigated, which are a function of the conjugation length. The time dependent density functional (TD-DFT) studies were performed to understand and support the experimental findings. The LUMO could be significantly stabilized by increasing the conjugation. The thermal stability of Fc-TPA **3a–3c** can be improved by increasing the conjugation length. The single crystal X-ray structure of Fc-TPA **3a** is reported, which show interesting supramolecular interactions leading to the formation of 2D-network.

Keywords: Sonogashira cross-coupling. Photophysical. Electrochemical. TD-DFT studies.

Introduction:

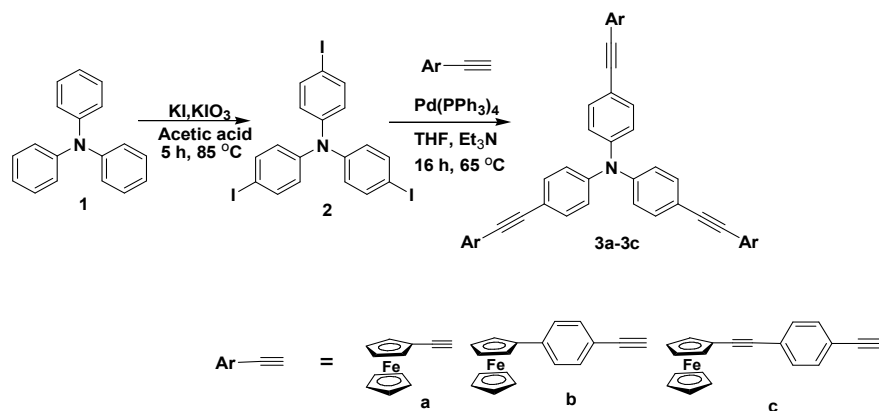
There has been continuous growing research interest on the triphenylamine derivatives due to their low oxidation potential, and hole transport properties.¹ The triphenylamine derivatives have been widely explored in Organic light-emitting diodes (OLEDs), Organic field-effect transistors (OFETs), Nonlinear Optics (NLO) and Dye-sensitized solar cells (DSSCs).² The literature reveals that the photonic properties of the triphenylamine can be tuned by the peripheral modifications.³

Our group has explored ferrocene as a strong donor, when incorporated into a variety of molecular systems.⁴⁻⁶ Lin *et al.* have synthesized polyferrocene based thiophene and triphenylamine.⁷ We were interested to incorporate the ferrocenyl moiety with varying spacer lengths on the periphery of triphenylamine and to explore its electron donating behavior. The literature reveals that there are limited number of reports, where the synergistic effect of donor on its photonic properties were explored.⁸

In continuation of our work on ferrocenyl functionalized triphenylamine derivatives, we were interested to design and synthesize C₃-symmetric ferrocenyl-triphenylamines with systematic variation of the conjugation length.

Results and discussion.

The ferrocenyl substituted triphenylamine conjugates (Fc-TPA) **3a–3c** were synthesized by the Pd-catalyzed Sonogshira cross-coupling reaction (Scheme 1).⁹ The intermediate *tris*-(4-iodo-phenyl)-amine **2** was synthesized by the iodination reaction of triphenylamine (**1**) using KI, KIO₃ as reagent, and acetic acid as a solvent for 5 h, in 80% yield.¹⁰ The Sonogshira cross-coupling reaction of the *tris*-(4-iodo-phenyl)-amine (**2**) with the corresponding alkynyl-ferrocenes (**a**, **b** and **c**) in the presence of Pd(PPh₃)₄ and CuI as a co-catalyst, and tetrahydrofuran (THF) as a solvent resulted in the homo-coupling product. Therefore the reaction was performed in the absence of copper-iodide (CuI). The Sonogashira cross-coupling reaction of *tris*-(4-iodo-phenyl)-amine **2** with ethynylferrocene (**a**), 1-ferrocene-4-ethynyl-benzene (**b**), and 1-ferrocenyl-1-ynyl-4-ethynyl-benzene (**c**), were performed using Pd(PPh₃)₄ as catalyst, and triethylamine as a base, which resulted Fc-TPA **3a–3c** in ~70% yield (Scheme 1).



Scheme 1. Synthesis of Fc-TPA **3a–3c**.

The Fc-TPA **3a–3c** were purified by column chromatography and well characterized by ¹H, ¹³C NMR, and HRMS techniques. The Fc-TPA **3a** was also characterized by single crystal X-ray diffraction technique. The ¹H NMR spectrum of the Fc-TPA **3a–3c** shows a characteristic doublet in the region 7.56–7.40 ppm corresponding to phenyl rings of the triphenylamine core. In Fc-TPA **3a–3c** monosubstituted cyclopentadienyl rings of the ferrocene exhibits a triplet between 4.69–4.51 ppm, whereas the unsubstituted cyclopentadienyl ring of the ferrocene exhibits a multiplet in the region 4.28–4.06 ppm.

The thermal properties of the Fc-TPA **3a–3c** were explored using thermogravimetric analysis (TGA) at a heating rate of $10\text{ }^{\circ}\text{C min}^{-1}$ under nitrogen atmosphere (Figure S18). The decomposition temperature for 5% weight loss in the Fc-TPA **3a–3c** were found to be $180\text{ }^{\circ}\text{C}$, $248\text{ }^{\circ}\text{C}$, $334\text{ }^{\circ}\text{C}$ respectively. This reflects the thermal stability of Fc-TPA **3a–3c** is directly proportional to the conjugation length.

X-ray analysis:

The single crystal of Fc-TPA **3a** was obtained via slow evaporation of dichloromethane solution at room temperature, which crystallizes into centrosymmetric monoclinic space group P21/n. The cyclopentadienyl rings of the ferrocenyl moieties show skew-eclipsed conformation (Figure 1). The dihedral angles between the planes containing the triphenylamine core, and the cyclopentadienyl ring of the ferrocenyl groups (Fc 1), (Fc 2), and (Fc 3) were found to be 17.74° , 15.43° and 17.74° respectively. The important bond lengths and bond angles are listed in Table S1.

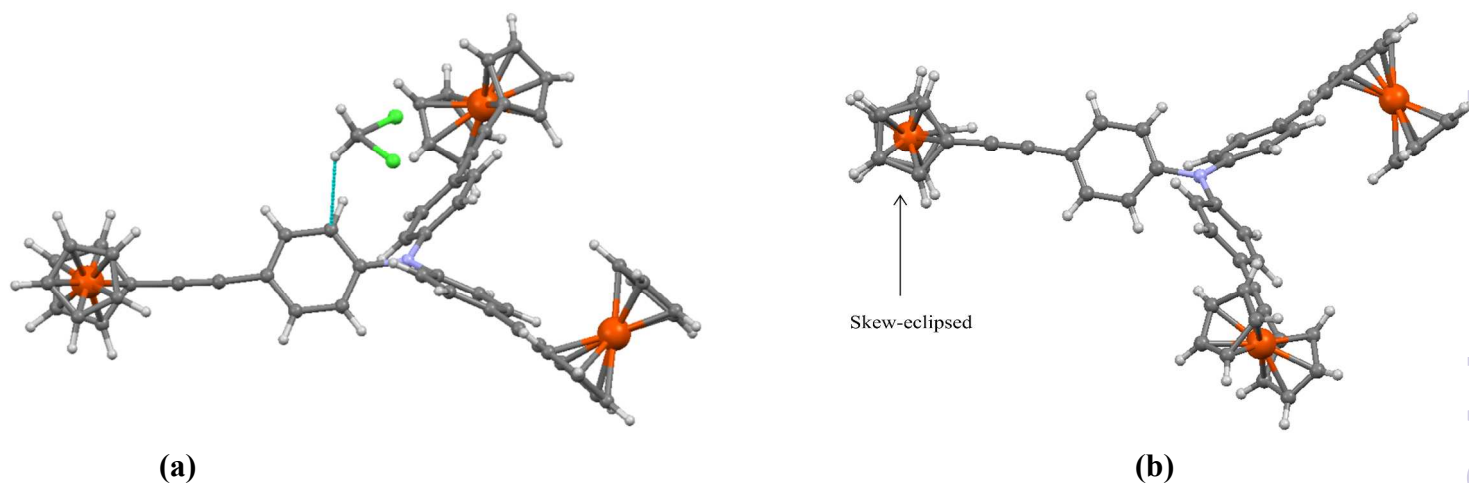


Figure 1. Single crystal X-ray structure of the Fc-TPA **3a** (a) through *a*-axis (dichloromethane solvent molecule) and (b) through *b*-axis (Skew-eclipsed conformation).

The crystal packing diagram of the Fc-TPA **3a** reveals, intermolecular $C_{cp}-H \cdots \pi$ interactions between the two adjacent molecules, which are interconnected via two different $C_{cp}-H \cdots \pi$ interactions. The $C-H \cdots \pi$ interaction between hydrogen (H21) and ferrocenyl cyclopentenyl ring (C50–C55, 3.29 Å) results in the formation of a dimer. The $C-H_{cp} \cdots \pi$ interactions between hydrogen (H42) of the ferrocenyl cyclopentenyl ring and the phenyl ring (C9–C14, 3.04 Å) leads to the formation of 2-D network (Figure 2).

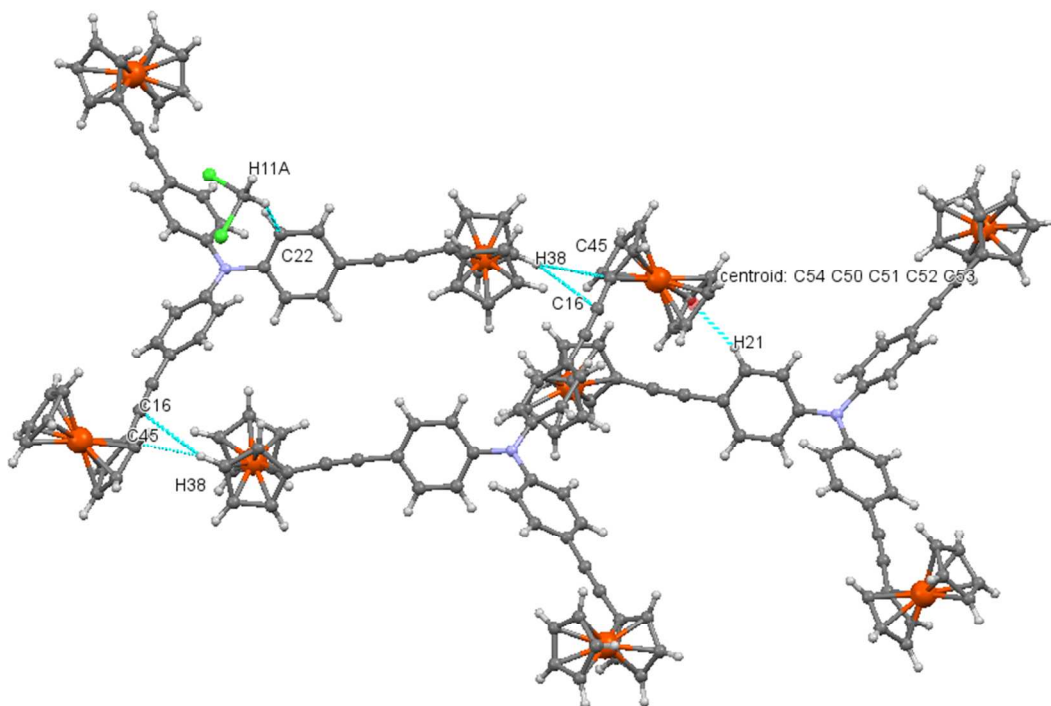


Figure 2. Packing diagram of Fc-TPA **3a**, forming 2-D network through *b*-axis. The secondary interactions are shown by the dashed lines.

Photophysical properties.

The electronic absorption spectra of Fc-TPA **3a–3c** were recorded in dichloromethane at room temperature, and the photophysical data are listed in Table 1. The Fc-TPA **3a–3c** show strong absorption band between 368–386 nm corresponding to $\pi \rightarrow \pi^*$ transition. (Figure 3).¹¹ The red shift in the absorption maxima for $\pi \rightarrow \pi^*$ absorption band follows the order **3c** > **3b** > **3a**. The variation in colors of the Fc-TPA **3a–3c** in dichloromethane is shown in Figure S10.

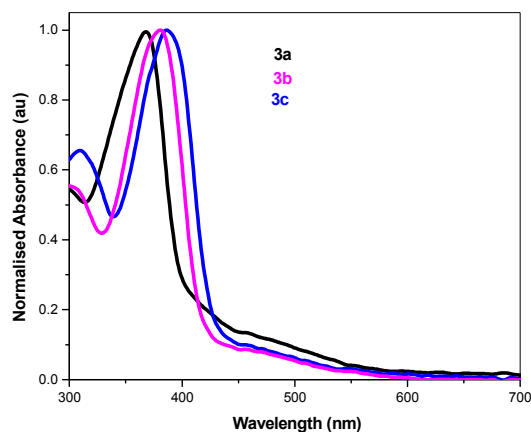


Figure 3. Normalized electronic absorption spectra of the Fc-TPA **3a–3c** in CH_2Cl_2 (1.0×10^{-4} M).

Electrochemistry

The electrochemical behavior of the Fc-TPA **3a–3c** were investigated by the cyclic voltammetric (CV) analysis in dry dichloromethane (DCM) solution at room temperature using tetrabutylammoniumhexafluorophosphate (TBAPF_6) as a supporting electrolyte. The electrochemical data of Fc-TPA **3a–3c** are listed in Table 1 and the representative cyclic voltammogram is shown in Figure S11. The cyclic voltammograms of the Fc-TPA **3a–3c** show two oxidation waves. The first reversible oxidation wave corresponding to ferrocene moiety at $E_{1/2} = 0.06\text{--}0.07$ V, and second reversible oxidation wave corresponding to triphenylamine unit $E_{1/2} = 0.72\text{--}0.78$ V.¹² The oxidation potential of the ferrocene unit in Fc-TPA **3a–3c** follows the order **3c** > **3b** > **3a**.

Table 1. Photophysical, and electrochemical properties of compounds 3a-3c.

Compounds	λ_{\max} [nm] (ϵ [Lmol ⁻¹ cm ⁻¹]) ^a	E _{oxid} (V)	Optical HOMO–LUMO gap (eV) ^d
3a	368 (31000)	0.06 ^b 0.72 ^c	3.02
3b	381(13466)	0.07 ^b 0.74 ^c	2.85
3c	386 (48000)	0.07 ^b 0.78 ^c	2.78
Ferrocene	-	0.00	-

^aMeasured in dichloromethane. ^b The oxidation value of ferrocene unit, and ^c the oxidation value of triphenylamine unit. ^dOptical HOMO–LUMO gap estimated from the absorption edge.

Computational Details.

In order to understand the photophysical and electrochemical properties of the Fc-TPA **3a–3c**, the time dependent density functional calculations (TD-DFT) were performed.¹³ All the quantum chemical calculations were performed using the Gaussian 09 program.¹⁴ The structures (**3a–3c**) were optimized using CAM–B3LYP to understand their photophysical properties.^{15,16} The solvent calculations were carried out in the dichloromethane (DCM) using the polarized continuum model (PCM)¹⁷ as implemented into Gaussian 09 software. The 6–31G** basis set for C, N, H and LANL2DZ for Fe was used for all the calculations. The excitation energies were calculated by the TD-DFT approach with the lowest 600 singlet excited states to cover the 300–750 nm range of UV–vis spectra. All the UV–vis spectra computed at PCM–TDDFT were extracted from Gaussian output file using the Gaussview 5.0 program.¹⁶

The calculated (DFT) structural parameters of Fc-TPA **3a** agree well with the experimental data (Figure 4). The optimized structure of Fc-TPA **3a** show eclipsed conformation of cyclopentadienyl rings of the ferrocenyl groups, whereas the crystal structure shows Skew-eclipsed conformation (Figures S12).

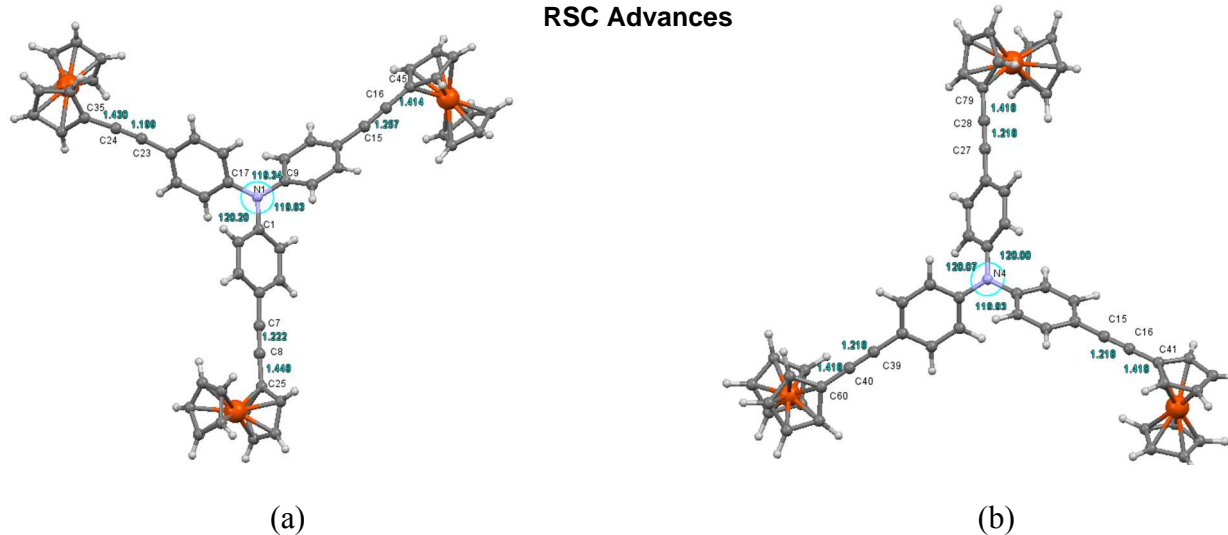


Figure 4. Comparison of selected bond lengths of (a) crystal structure and (b) CAM-B3LYP optimized structure of Fc-TPA **3a**.

Time dependent density functional (TD-DFT) studies:

In order to determine the nature of the excited states of Fc-TPA **3a–3c**, the time dependent-density functional theory (TD-DFT) calculations were carried out. The experimental (UV-vis) and computed (TD-DFT: CAM-B3LYP) absorption spectra are shown in Figure 5. The Fc-TPA **3a**, **3b** and **3c** show strong absorption band calculated at 327 nm, 344 nm, and 358 nm with good oscillator strengths of 1.4958, 1.7963, and 2.9417 respectively. The experimental values for these transition are 368, 381, 386 nm for **3a**, **3b** and **3c** respectively. Therefore, the experimental and calculated trends are similar. The molecular orbitals (MOs) associated to these transition confirms the $\pi \rightarrow \pi^*$ transition (Figures S13 and S14).

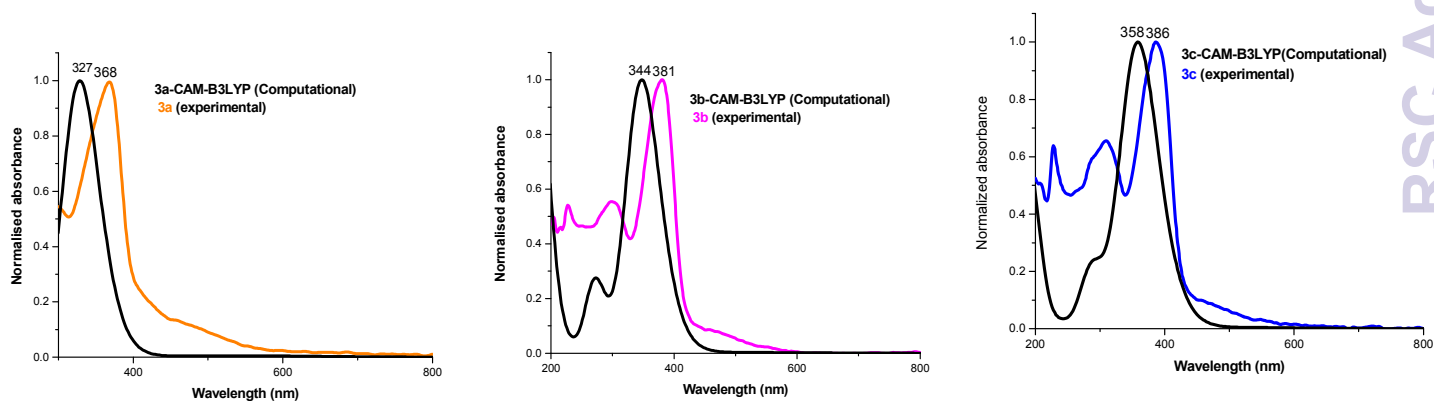


Figure 5. The comparison of experimental and calculated (TD-DFT at CAM-B3LYP level) absorption spectrum of Fc-TPA **3a–3c** in DCM solution.

In Fc-TPA **3a–3c** shows the HOMO→LUMO transition contributes to the lowest excited state by 73%, 38%, and 43% respectively as shown in Table 2. Thus, the lowest excited states of Fc-TPA **3a–3c** are assign to the $\pi\rightarrow\pi^*$ absorption band which was further conformed by molecular orbitals of HOMO→LUMO.

Table 2. Computed vertical transition energies and their Oscillator strengths (f) and Major contributions for the Fc-TPA **3a–3c**.

Fc-TPA 3a–3c	TD-DFT/ CAM-B3LYP (DCM)		
	λ_{\max}	f	Major contribution (%)
1	327 nm	1.4958	HOMO→LUMO (73%)
2	344 nm	1.7963	HOMO→LUMO (38%)
3	358 nm	2.9417	HOMO→LUMO (43%)

Conclusions

In summary, we have described the synthesis of ferrocenyl functionalized triphenylamines. The photonic, electronic, and thermal properties of the triphenylamines can be tuned by varying the spacer length. These results show the design of new materials with varying spacers for various optoelectronic applications. The optical and electrochemical properties of the materials are explained from the TD-DFT calculations. The results obtained here will be helpful in design of molecular systems for photonic applications. The optical limiting properties of these materials are currently ongoing in our laboratory.

Experimental section

General experimental. All reagents were obtained from commercial sources, and used as received unless otherwise stated. ^1H NMR (400 MHz) and ^{13}C NMR (100 MHz) spectra were recorded on a Bruker Avance (III) 400 MHz instrument by using CDCl_3 as solvent. ^1H NMR chemical shifts are reported in parts per million (ppm) relative to the solvent residual peak (CDCl_3 , 7.26 ppm). Multiplicities are given as s (singlet), d (doublet), t (triplet), q (quartet), dd (doublet of doublets), and m (multiplet), and the coupling constants, J , are given in Hz. ^{13}C NMR chemical shifts are reported relative to the solvent residual peak (CDCl_3 , 77.36 ppm). Thermogravimetric analyses were performed on the Mettler Toledo Thermal Analysis system. UV–visible absorption spectra were recorded on a Cary-100 Bio UV–visible spectrophotometer. Cyclic voltamograms (CVs) were recorded on a CHI620D electrochemical analyzer using glassy carbon as the working electrode, Pt wire as the counter electrode, and the saturated calomel electrode (SCE) as the reference electrode. The scan rate was 100 mV s^{-1} . A solution of tetrabutylammonium hexafluorophosphate (TBAPF6) in CH_2Cl_2 (0.1 M) was employed as the supporting electrolyte. DCM was freshly distilled from CaH_2 prior to use. All potentials were experimentally referenced against the saturated calomel electrode couple but were then manipulated to be referenced against Fc/Fc^+ as recommended by IUPAC. Under our conditions, the Fc/Fc^+ couple exhibited $E^\circ = 0.38\text{ V}$ versus SCE. HRMS was recorded on a Bruker-Daltonics micrOTOF-Q II mass spectrometer. The single crystal X-ray structure of the Fc-TPA **3a** CCDC number is 995106.

X-ray crystallography. Single crystal X-ray structural studies of **3a** were performed on a CCD Agilent Technologies (Oxford Diffraction) SUPER NOVA diffractometer. Data were collected at 293(2) K using graphite-monochromated $\text{Cu K}\alpha$ radiation ($\lambda_\alpha = 1.54184\text{ \AA}$). The strategy for the Data collection was evaluated by using the CrysAlisPro CCD software. The data were collected by the standard ϕ - ω scan techniques, and were scaled and reduced using CrysAlisPro RED software. The structures were solved by direct methods using SHELXS-97 and refined by full matrix least-squares with SHELXL-97, refining on F^2 .¹

The positions of all the atoms were obtained by direct methods. All non-hydrogen atoms were refined anisotropically. The remaining hydrogen atoms were placed in geometrically constrained positions and refined with isotropic temperature factors, generally $1.2U_{eq}$ of their

parent atoms. The crystal and refinement data are summarized in Table S2, and selected bond distances and bond angles are shown in Table S3.

General Procedure for the preparation of Fc-TPA 3a-3c

In the presence of argon atmosphere a solution of tris-(4-iodo-phenyl)-amine **2** (0.2 g, 0.38 mmol) and the corresponding ethynyl ferrocene (4 equivalent) in dry THF (20ml), added triethylamine (5 ml), Pd(PPh₃)₄ (0.100 g, 0.08 mmol), stirred for 16 h at 65 °C, after completion of the reaction, the reaction mixture was concentrated under reduced pressure, the crude compound was purified by column chromatography on silica, using Hexane/ DCM (60:40), and afforded pure compounds **3a-3c** around 70 % yield.

Fc-TPA 1. Fc-TPA 3a. Orange solid (0.231 g, 69 %) Mp > 250 °C. ¹H NMR (CDCl₃, 400 MHz, ppm): δ 7.40 (d, J = 8 Hz, 6H, Ph), 7.06 (d, J = 8 Hz, 6H, Ph), 4.51 (t, 6H, Cp'), 4.26 (t, 19H, Cp' and Cp). ¹³C NMR (CDCl₃, 100 MHz, ppm): 146.2 (Ph), 132.5 (Ph), 123.9 (Ph), 118.5 (Ph), 88.0 (C≡C), 71.3 (Cp), 69.9 (Cp'), 68.7 (Cp), 65.4 (Cp). HRMS (ESI-TOF): m/z calculated for C₅₄H₃₉Fe₃N 869.1067 [M]⁺, measured 869.1141 [M]⁺.

Fc-TPA 3b. Orange solid (0.297 g, 70%) Mp > 280 °C. ¹H NMR (CDCl₃, 400 MHz, ppm): δ 7.56 (s, 18H, Ph), 7.12 (d, J = 8 Hz, 6H, Ph), 4.69 (s, 5H, Cp'), 4.37 (s, 6H, Cp' and Cp), 4.06 (s, 13H, Cp' and Cp). ¹³C NMR (CDCl₃, 100 MHz, ppm): 145.5 (Ph), 138.7 (Ph), 131.7 (Ph), 130.5 (Ph), 127.3 (Ph), 124.8 (Ph), 123.0 (Ph), 119.4 (Ph), 117.1 (Ph), 88.6 (Ph), 88.3 (Ph), 83.2 (C≡C), 68.7 (Cp'), 68.3 (Cp'), 65.4 (Cp). HRMS (ESI-TOF): m/z calculated for C₇₂H₅₁Fe₃N 1097.2071 [M]⁺, measured 1097.2078 [M]⁺.

Fc-TPA 3c. Orange solid (0.31 g, 75%) Mp > 300 °C. ¹H NMR (CDCl₃, 400 MHz, ppm): δ 7.47 (d, J = 12 Hz, 18H, Ph), 7.11 (d, J = 8 Hz, 6H, Ph), 4.53 (t, 5H, Cp'), 4.28 (t, 17H, Cp). ¹³C NMR (CDCl₃, 100 MHz, ppm): 146.7 (Ph), 132.8 (Ph), 131.4 (Ph), 131.3 (Ph), 124.0 (Ph), 123.7 (Ph), 122.5 (Ph), 117.8 (Ph), 90.8 (Ph), 90.5 (Ph), 89.3 (Ph), 85.6 (C≡C), 71.4 (C≡C), 70.0 (Cp'), 69.0 (Cp'), 64.9 (Cp). HRMS (ESI-TOF): m/z calculated for C₇₈H₅₁Fe₃N 1169.2072 [M]⁺, measured 1169.2079 [M]⁺.

Supporting Information

The ^1H NMR, ^{13}C NMR spectra, mass spectroscopy data, cyclic voltammograms, UV-vis graphs, and DFT calculations of Fc-TPA **3a-3c** are provided.

Corresponding Author

*E-mail: rajneeshmisra@iiti.ac.in.

Tel.: +91 7312438710; fax: +91 7312361482.

Acknowledgements

The work was supported by DST, and CSIR Govt. of India, New Delhi. We are grateful to the Sophisticated Instrumentation Centre (SIC), IIT Indore.

References

- 1 N. Metri, N. X. Sallenave, C. Plesse, L. Beouch, P. H. Aubert, F. Goubard, C. Chevrot, and G. Sini. *J Phys. Chem. C.*, 2012, **116**, 3765–3772.
- 2 (a) M. Szablewski, P. R. Thomas, A. Thornton, D. Bloor, G. H. Cross, J. M. Cole, J. A. K Howard, M. Malagoli, F. Meyers, J. L. Bredas, W. Wenseleers, and E. Goovaerts. *J. Am. Chem. Soc.*, 1997, **119**, 3144–3154; (b) S. Barlow, and S. R. Marder. *Chem. Commun.* 2000, 1555–1562; (c) J. L. Segura, and N. Martin. *Angew. Chem. Int. Ed.* **2001**, *40*, 1372–1409; (d) R. R. Tykwinski, U. Gubler, R. E. Martin, F. Diederich, C. Bosshard, and P. Gunter. *J. Phys. Chem. B.*, 1998, *102*, 4451–4465.
- 3 (a) J. Y. Kim, K. Lee, N. E. Coates, D. Moses, T. Q. Nguyen, M. Dante, and A. J. Heeger, *Science*, 2007, **317**, 222; (b) G. Dennler, M. C. Scharber, and C. Brabec, *Adv. Mater.*, 2009, **21**, 1323.
4. (a) C. J. Ziegler, K. Chanawanno, A. Hasheminsasab, Y. U. Zatsikha, E. Maligaspe, and V. N. Nemykin. *Inorg. Chem.*, 2014, **53**, 4751-4755; (b) R. Misra, B. Dhokale, T. Jadhav, and S. M. Mobin. *Dalton Trans.*, 2014, **43**, 4854; (c) R. Misra, B. Dhokale, T. Jadhav, and S. M. Mobin. *Organometallics*, 2014, **33**, 1867–1877; (d) R. Maragani, and R. Misra. *Tetrahedron*, 2014, **70**, 3390-3399; (e) V. Nemykin, A. Y. Maximov, and A. Y. Kopusov,

- Organometallics*, 2007, **26**, 3138-3148. (f) X. Tang, W. Liu, J. Wu, C. S. Lee, J. You, And P. Wang. *J. Org. Chem.*, 2010, **75**, 7273–7278; (g) B. Breiten, M. Jordan, D. Taura, M. Zalibera, M. Griesser, D. Confortin, C. Boudon, J. P. Gisselbrecht, W. B. Schweizer, G. Gescheidt, and F. Diederich. *J. Org. Chem.*, 2013, **78**, 1760–1767.
- 5 (a) S. R. Marder, B. Kippelen, A. K. Y. Jen, and N. Peyghambarian. *Nature*, 1997, **388**, 845–851; (b) B. Fabre. *Acc. Chem. Res.*, 2010, **43**, 1509; (c) J. H. R. Tucker, and S. R. Collinson. *Chem. Soc. Rev.*, 2002, **31**, 147.
- 6 (a) P. Gautam, B. Dhokale, V. Shukla, C. P. Singh, K. S. Bindra, and R. Misra. *J. Photochem. Photobiol. A.*, 2012, **239**, 24–27; (b) R. Maragani, T. Jadhav, S. M. Mobin, and R. Misra. *Tetrahedron*, 2012, **68**, 7302–7308; (c) B. Dhokale, P. Gautam, S. M. Mobin, and R. Misra, *Dalton Trans.*, 2013, **42**, 1512–1518; (d) R. Maragani, T. Jadhav, S. M. Mobin, and R. Misra *RSC Adv.* 2013, **3**, 2889–2892; (e) R. Misra, P. Gautam, R. Sharma, and S. M. Mobin, *Tetrahedron Lett.*, 2013, **54**, 381–383; (f) T. Jadhav, R. Maragani, R. Misra, V. Sreeramulu, D. N. Rao, and S. M. Mobin. *Dalton Trans.*, 2013, **42**, 4340–4342; (g) R. Misra, P. Gautam, T. Jadhav, S. M. Mobin, *J. Org. Chem.* 2013, **78**, 4940–4948; (h) R. Sharma, R. Maragani, S. M. Mobin, and R. Misra. *RSC Adv.*, 2013, **3**, 5785; (i) R. Maragani, and R. Misra. *Tetrahedron Lett.*, 2013, **54**, 5399–5402; (j) R. Misra, T. Jadhav, and S. M. Mobin. *Dalton Trans.*, 2014, **43**, 2013–2022; (k) R. Misra, R. Sharma, and S. M. Mobin. *Dalton Trans.*, 2014, **43**, 6891–6896; (l) R. Misra, B. Dhokale, T. Jadhav, and S. M. Mobin. *Dalton Trans.*, 2013, **42**, 13658; (m) R. Misra, R. Maragani, T. Jadhav, and S. M. Mobin. *New j. Chem.* 2014, **38**, 1446-1457.
- 7 (a) S. Kato, M. Kivala, W. B. Schweizer, C. Boudon, J. P. Gisselbrecht, and F. Diederich. *Chem. Eur. J.*, 2009, **15**, 8687-8691; (b) T. Michinobu, J. C. May, J. H. Lim, C. Boudon, J. P. Gisselbrecht, P. Seiler, M. Gross, I. Biaggio, and F. Diederich. *Chem. Commun.*, 2005, 737–739. (c) M. Kivala, C. Boudon, J. P. Gisselbrecht, P. Seiler, and F. Diederich. *Chem. Commun.*, 2007, 4731–4733; (d) M. Kivala, F. Diederich. *Acc. Chem. Res.*, 2009, **42**, 235–248. (e) S. i. Kato, F. and Diederich, *Chem. Commun.*, 2010, **46**, 1994–2006; (f) R. Misra, P. Gautam, and T. Jadhav, *J. Org. Chem.*, 2013, **78**, 12440–12452; (g) P. Gautam, R. Maragani, and R. Misra. *Tetrahedron*

- Lett.*, 2014, **55**, 6827–6830; (h) R. Misra, R. Maragani, K. R. Patel, and G. D. Sharma. *RSC Adv.* 2013, **3**, 2889–2892.
- 8 R. Misra, B. Dhokale, and T. Jadhav. *RSC Adv.*, 2015, **5**, 57692-57699.
- 9 K. R. J. Thomas, and J. T. Lin. *J. Organomet. Chem.* 2001, 139–144.
- 10 C. Sissa, V. Parthasarathy, D. D. Kucma, M. H. V. Werts, M. B. Desce, and F. Terenziani, *Phys. Chem. Chem. Phys.*, 2010, **12**, 11715–11727.
- 11 V. N. Nemykin, E. A. Makarova, J. O. Grosland, R. G. Hadt, and A. Y. Kuposov. *Inorg. Chem.* 2007, **46**, 9591-9601.
- 12 (a) B. Dhokale, P. Gautam, and R. Misra. *Tetrahedron Lett.*, 2012, **53**, 2352–2354; (b) V. A. Nadtochenko, N. N. Denisov, V. Y. Gak, N. V. Abramova, and N. M. Loim. *Russ. Chem. Bull*, 1999, **148**, 1900–1903; (c) S. Barlow, and S. R. Marder. *Chem. Commun.*, 2000, 1555–1562; (d) R. Sharma, P. Gautam, S. M. Mobin, and R. Misra. *Dalton Trans.* 2013, **42**, 5539–5545.
- 13 (a) C. Teng, X. Yang, C. Yang, S. Li, M. Cheng, A. Hagfeldt, and L. Sun. *J. Phys. Chem. C.*, 2010, **114**, 9101–9110; (b) C. Sakong, H. J. Kim, S. H. Kim, J. W. Namgoong, J. H. Park, J. H. Ryu, B. Kim, M. J. Kob, and J. P. Kim. *New J. Chem.*, 2012, **36**, 2025–2032.
- 14 (a) T. Mochida, and S. Yamazaki. *J. Chem. Soc. Dalton Trans.*, 2002, 3559–3564; (b) T. Michinobu, H. Kumazawa, K. Noguchi, and K. Shigehara, *Macromolecules* 2009, **42**, 5903–5905.
- 15 (a) W. W. Zhang, Y. G. Yu, Z. D. Lu, W. L. Mao, Y. Z. Li, and Q. J. Meng. *Organometallics* 2007, **26**, 865-873; (b) A. D. J. Becke. *J. Chem. Phys.* 1993, **98**, 5648-5652; (b) C. T. Lee, W. T. Yang, and R. G. Parr. *Phys. Rev. B.*, 1988, **37**, 785-789; (c) P. J. Hay, W. R. Wadt. and *J. Chem. Phys.* 1985, **82**, 270-283.
- 16 A. Pedone. *J. Chem. Theory Comput.* 2013, **9**, 4087–4096; (b) D. G. Gusev. *Organometallics* 2013, **32**, 4239–4243.

- 17 (a) M. M. Francl, W. J. Pietro, W. J. Hehre, J. S. Binkley, M. S. Gordon, D. J. Defrees, and J. A. Pople, *J. Chem. Phys.* 1982, **77**, 3654-3665; (b) F. Ding, S. Chen, H. Wang. *Materials* 2010, **3**, 2668-2683.